Resonant X-Ray Diffraction Study of an Unusually Large Phase Coexistence in Smectic Liquid-Crystal Films

LiDong Pan, P. Barois, R. Pindak, Z. Q. Liu, B. K. McCoy, and C. C. Huang

Resonant X-ray Diffraction Study of Unusually Large Phase Coexistence in Smectic Liquid Crystal Films

LiDong Pan,[1,2] P. Barois,[3] R. Pindak,[4] Z. Q. Liu,[5] B. K. McCoy,[6] and C. C. Huang[1]

[1]School of Physics and Astronomy, University of Minnesota, Minneapolis, Minnesota 55455, USA
[2]Department of Physics and Astronomy, Johns Hopkins University, Baltimore, Maryland 21218, USA
[3]Centre de Recherche Paul Pascal, Université de Bordeaux, CNRS, 33600 Pessac, France
[4]Photon Sciences Directorate, Brookhaven National Laboratory, Upton, New York 11973, USA
[5]Department of Chemistry and Physics, St. Cloud State University, St. Cloud, Minnesota 56301, USA
[6]Department of Mathematics and Physics, Azusa Pacific University, Azusa, California 91702, USA

The recent discovery of the new smectic-C_{d6}^* ($\mathrm{Sm}C_{d6}^*$) phase [S. Wang *et al.*, *Phys. Rev. Lett* **104**, 027801 (2010)] also revealed the existence of a *noisy region* in the temperature window between the $\mathrm{Sm}C_{d6}^*$ phase and the smectic-C_{d4}^* ($\mathrm{Sm}C_{d4}^*$) phase. Characterized by multiple resonant peaks spanning a wide region in Q_Z, the corresponding structure of this temperature window has been a mystery. In this paper, through a careful resonant x-ray diffraction study and simulations of the diffraction spectra, we show that this region is in fact an unusually large coexistence region of the $\mathrm{Sm}C_{d6}^*$ phase and the $\mathrm{Sm}C_{d4}^*$ phase. The structure of the noisy region is found to be a heterogeneous mixture of local $\mathrm{Sm}C_{d6}^*$ and $\mathrm{Sm}C_{d4}^*$ orders on the sub-μm scale.

Structural determination is an important step in understanding material properties. Scattering experiments are the most widely used method for this purpose [1]. However, when disordered or non-periodic structures are involved, it can be a very demanding and challenging task to find out the atomic or molecular arrangements of the samples under study [2]. For soft materials, where partial positional order and/or orientational order are observed, structural elucidation in the presence of disorder is even more complicated.

Antiferroelectric liquid crystals (AFLC) present an interesting class of materials that show several different smectic-C^* ($\mathrm{Sm}C^*$) variant phases in a relatively narrow temperature window [3, 4]. In $\mathrm{Sm}C^*$ type phases, elongated organic molecules are arranged in layers and the long molecular axes are tilted away from the layer normal (Z axis). The tilt magnitude is constant across the bulk sample, while the tilt directions can be different in different layers. The different azimuthal arrangements of the tilt direction along the Z axis distinguish different $\mathrm{Sm}C^*$ variant phases. For example, the $\mathrm{Sm}C_\alpha^*$ phase has an incommensurate helical tilt structure, while the $\mathrm{Sm}C_{d4}^*$ phase has a biaxial *distorted clock structure* with a 4 layer periodicity along the Z direction [5–7].

Recently a new $\mathrm{Sm}C^*$ variant phase, the $\mathrm{Sm}C_{d6}^*$ phase, was discovered [8]. This phase is characterized by a biaxial distorted clock structure with a periodicity of 6 layers along the Z direction. In the resonant x-ray diffraction (RXRD) experiments that revealed its existence, a *noisy region* right below the $\mathrm{Sm}C_{d6}^*$ phase was also identified. This region is characterized by multiple resonant peaks spanning a wide range in Q_Z in the RXRD experiments. Elucidation of the structure of the noisy region through RXRD experiments and simulation of the diffraction spectra is the main purpose of this paper.
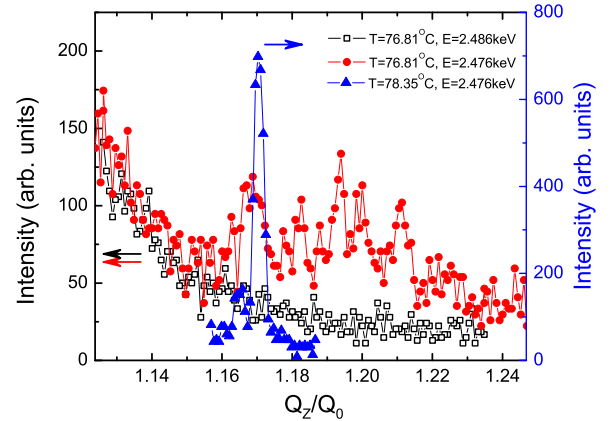

FIG. 1: (Color online) Sample scan data of the RXRD experiments. Resonant scans in the noisy region (red dots, T = 76.81°C) and the $\mathrm{Sm}C_{d6}^*$ phase (blue triangles, T = 78.35°C) as well as off-resonant scan in the noisy region (black squares) are shown as a function of Q_Z/Q_0. Note the $\mathrm{Sm}C_{d6}^*$ scan is shown on a different scale (right axis).

The sample studied is a mixture of 11% C11 and 89 % 10OHF by weight percentage. The chemical structures of C11 and 10OHF can be found in Ref. [8], Fig. 1. It is one of the mixtures from which the $\mathrm{Sm}C_{d6}^*$ phase was first discovered (*Mixture B* in Ref. [8]). This batch of sample shows a phase sequence, $\mathrm{Sm}A$ (89.5°C) $\mathrm{Sm}C_\alpha^*$ (78.6°C) $\mathrm{Sm}C_{d6}^*$ (77.5°C) *Noisy Region* (75.6°C) $\mathrm{Sm}C_{d4}^*$ upon cooling.

The RXRD experiments were carried out at beam line X19A in National Synchrotron Light Source, Brookhaven National Laboratory. To date, RXRD remains the only technique that can measure the orientational periodicity of the $\mathrm{Sm}C^*$ variant phases directly [6, 8–10]. Since those phases are characterized by different unit cell (u.c.) sizes,

measurement of this quantity is essential for phase identification and structure elucidation for AFLCs. At the resonant energy of the sulphur atom in the C11 molecule ($E_0 = 2.476$keV), satellite peaks appear in the Q-scan in addition to the Bragg peaks from the smectic layer structures [10]. The Bragg peaks appear at integer multiples of $Q_0 = 2\pi/$d, where d is the layer spacing. Then size of the u.c. can be determined from the relative positions of the satellite peaks and the Bragg peak. For example, the $\mathrm{Sm}C_{d6}^*$ is identified by the observation of resonant peaks around $Q_Z/Q_0 = 7/6$ (1.17), and the $\mathrm{Sm}C_{d4}^*$ phase shows resonant peaks around $Q_Z/Q_0 = 5/4$ (1.25).

A thick free standing film of the mixture was prepared in a two-stage oven with He exchange gas [11]. From the polarizing optical microscopy image and the Bragg peak intensities, the thickness of the film was estimated to be of several thousand layers. All the data presented in this paper were collected from this film. Details of the RXRD experiments have been reported elsewhere [9].

A resonant scan of the sample in the noisy region (T = 76.81°C) is shown in Fig. 1 as a function of Q_Z/Q_0. For comparison, an off-resonant scan (E = E_0+10eV) at the same temperature as well as a resonant scan in the $\mathrm{Sm}C_{d6}^*$ phase (T = 78.35°C) are also shown. From Fig. 1, it is clear that the scan in the noisy region shows multiple weak resonant peaks spanning a large window of Q_Z/Q_0. Although each individual peak is not necessarily wider than the resonant peaks of the $\mathrm{Sm}C_{d6}^*$ phase, the range of the resonant signal is much larger. It spans across the Q space from around $Q_Z/Q_0 = 1.16$ up to about $Q_Z/Q_0 = 1.24$, i.e., almost the entire region between the expected position of the $\mathrm{Sm}C_{d6}^*$ peaks and that of the $\mathrm{Sm}C_{d4}^*$ peaks. On the other hand, split resonant peaks due to a helical superstructure are clearly visible in the

FIG. 2: (Color online) RXRD spectra from the sample upon cooling plotted as a function of temperature and Q_Z/Q_0. Intensities of resonant signals are shown in logarithmic color scale. Non-resonant background intensities from the tails of the Bragg peaks have been subtracted.

$\mathrm{Sm}C_{d6}^*$ phase in Fig. 1, indicating a very good resolution in the Q_Z scan of our RXRD experiments.

In order to obtain a complete picture of the noisy region, scans were performed across this temperature window in a 30mK/step cooling run. The resulting spectra are shown in Fig. 2 in a contour plot. From Fig. 1, we find that the scans in the Q space of interest have a Q_Z dependent non-resonant background, which comes from the tail of the Bragg peak at $Q_Z/Q_0 = 1.00$. This non-resonant contribution was subtracted from the scans before they were plotted in Fig. 2 [12]. To account for the beam damage and chemical degradation of the sample, all the scans shown in Fig. 2 are normalized according to the integrated intensities of their corresponding Bragg peaks [13]. After these procedures, the data shown in Fig. 2 present only the resonant intensities related to the azimuthal structures of the sample as a function of temperature and Q_Z/Q_0.

Two major features can be observed in Fig. 2. First, as temperature is lowered across the noisy region, multiple resonant peaks are observed, while the center of those peaks gradually and consistently shifts toward higher Q_Z value. Second, the resonant peaks observed in the noisy region are all contained in between around $Q_Z/Q_0 = 1.16$ up to about $Q_Z/Q_0 = 1.24$. The main features of the scans in the noisy region are highly reproducible, i.e., although they do not overlap perfectly, intensity spectra obtained at the same temperature show the same overall shape.

On the other hand, the noisy region is thermodynamically stable. It appeared both in cooling as well as in heating. The features of the noisy region are reproduced in two RXRD cooling runs with different average cooling rates of 1K/hour and 2K/hour, respectively. In another mixture system (11.2% C9 mixed with 23.5% 11OHF and 65.3% 10OHF), the noisy region features right below the $\mathrm{Sm}C_{d6}^*$ phase remained clearly visible in a very slow cooling run over 16 hours, thus excluding the possibility that it is a non-equilibrium state.

Given the fact that the noisy region is found between the $\mathrm{Sm}C_{d6}^*$ phase and the $\mathrm{Sm}C_{d4}^*$ phase, together with the first order nature of the transition between those two phases, it is a reasonable postulation that the noisy region is a coexistence region of the $\mathrm{Sm}C_{d6}^*$ phase and the $\mathrm{Sm}C_{d4}^*$ phase. Meanwhile, in the polarizing optical microscopy set up on the sample oven during the RXRD experiments, no macroscopic phase separation or phase front motion was observed over this temperature window. Also, the evolutions of the resonant peaks are very different from what is expected of macroscopic phase coexistence (see Fig. 4 in Ref. [8] for example). Thus if this region is indeed a phase coexistence region, the coexisting structures must be mixed on a microscopic level.

To obtain a better understanding of the structure in the noisy region, we performed simulations of the RXRD spectra based on the model of tensorial structure factors
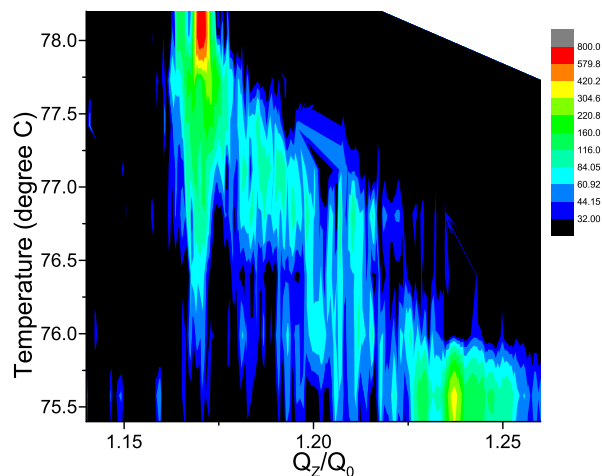
proposed by A.-M. Levelut and B. Pansu [10]. Two structural models of the microscopic coexistence of SmC_{d6}^* order and SmC_{d4}^* order are studied. In the models, we assume that the smallest structural elements are the u.c. of the SmC_{d6}^* phase and the SmC_{d4}^* phase. In other words, we assume the structure of the noisy region consists of mixtures of u.c. of the SmC_{d6}^* structure and of the SmC_{d4}^* structure. Each layer is assumed to belong to a certain structure and have the same tilt angle magnitude. Only complete u.c.s are put into the structural model with all the u.c. oriented along the same direction. [14]

Two scenarios of the coexistence structures are proposed. In the *nucleation model*, we assume that as temperature is lowered, the size of the SmC_{d6}^* regions shrink while the size of the SmC_{d4}^* regions grow. To reduce the parameters used in the model, an average nuclei size of 5 u.c. is assumed for the two structures. Each structure has a nuclei size that changes with temperature, e.g., when the SmC_{d6}^* structure has a nuclei size of 3 u.c., the

SmC_{d4}^* structure will have a nuclei size of 7 u.c. and those sizes change with temperature while the average is fixed at 5 u.c.. The two types of nuclei are distributed randomly along the Z direction with equal probabilities. In the *percolation model*, on the other hand, we assume that as temperature is lowered, the probability of finding a SmC_{d6}^* u.c. decreases while the probability of finding a SmC_{d4}^* u.c. increases [15]. Unit cells with different structures are randomly distributed along the Z direction in this model (i.e., the nuclei size is 1 u.c.).

The simulation results of the RXRD spectra based on the two scenarios are shown in Fig. 3. For the simulation, a 400 layer sample film with a 350 layer optical pitch is used. The optical pitch is necessary to produce split resonant peaks in the SmC_{d6}^* and the SmC_{d4}^* phase as observed in the experiments. The distortion angle used is $\pi/6$ for the SmC_{d6}^* structure and $\pi/3$ for SmC_{d4}^* [16]. Intensities of the resonant peaks are displayed in logarithmic color scale as a function of percentage of SmC_{d6}^* u.c. and Q_Z/Q_0. Higher percentage of SmC_{d6}^* u.c. corresponds to higher temperature in the experiment.

It is clear from Fig. 3 that both scenarios will produce multiple resonant peaks in a wide Q_Z region. However, they show very distinctive features. In the nucleation model, the resonant intensities are localized around the center of the Q_Z positions that correspond to the SmC_{d6}^* and SmC_{d4}^* structures [17]. As the SmC_{d6}^* percentage is lowered, the intensities around $Q_Z/Q_0 = 1.17$ decreases while the intensities around $Q_Z/Q_0 = 1.25$ increases. Although multiple resonant peaks are observed, the intensity near the center region around $Q_Z/Q_0 = 1.21$ is almost always zero.

For the percolation model, however, it is quite different. The spread out resonant intensities are not localized around either $Q_Z/Q_0 = 1.17$ or $Q_Z/Q_0 = 1.25$. Instead, multiple resonant peaks are observed across a much wider Q_Z region, with the center of those peaks shifting towards higher Q_Z value as the SmC_{d6}^* percentage decreases, which as explained above, corresponds to lowering of the temperature.

A comparison of the two models at 50% SmC_{d6}^* u.c. percentage illustrates their distinct behavior. Shown in Fig. 4(a) are the simulated scans of the SmC_{d6}^* phase and the SmC_{d4}^* phase, respectively. Figure 4(b) displays the results from the nucleation model and the percolation model with 50% SmC_{d6}^* (corresponding to a center horizontal cut of Fig. 3(a) and (b)). As shown, in the nucleation model the resonant intensities are mostly localized around the Q_Z region of the corresponding pure structures; while in the percolation model, the resonant intensities spread across a much wider Q_Z region.

Comparing the experimental RXRD spectrum to the simulation results presented in Fig. 3, it is clear that Fig. 3(b) is able to reproduce all the main features of the experiment, including the widespread multiple resonant peaks and the shifting of the intensity center as a
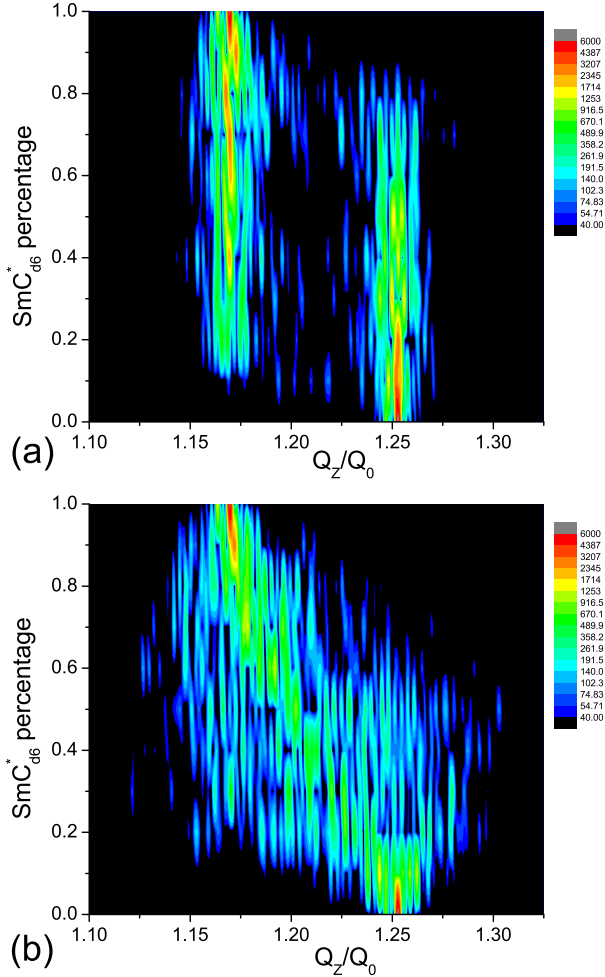

FIG. 3: (Color online) Simulated RXRD spectra from the (a) nucleation model and (b) percolation model plotted as a function of percentage of SmC_{d6}^* unit cells and Q_Z/Q_0. Intensities of resonant signals are shown in logarithmic color scale.
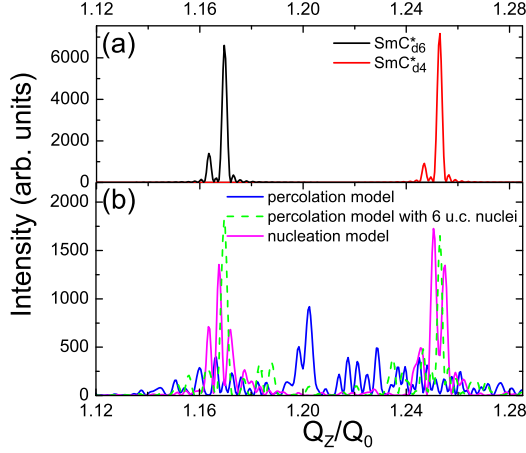
FIG. 4: (Color online) (a) Simulated resonant signals of the SmC_{d6}^* phase and the SmC_{d4}^* phase. (b) Simulated resonant signals from the noisy region of 50% unit cells with the SmC_{d6}^* structure and 50% with the SmC_{d4}^* structure from the nucleation model as well as the percolation model. Dashed line shows simulated intensities from percolation model with 6 unit cell nuclei sizes and 50% SmC_{d6}^*.

function of temperature. On the other hand, as shown in Fig. 4(b), when the percolation model is constructed with large nuclei clusters (6 u.c. size), the resulting spectrum show similar characteristics as the nucleation model, i.e., groups of peaks centered around $Q_Z = 1.17$ and 1.25 [18]. From those results, it is clear that to have wide spread resonant peaks, the mixed local structures must have very small correlation length (~ 1 u.c.). This qualitative result is independent of the model used. Thus the noisy region discovered in the RXRD experiments of AFLC mixtures is indeed a region of coexisting SmC_{d6}^* and SmC_{d4}^* order, with the two structures forming a percolating network on the sub-μm level.

The coexistence of two phases with a first order transition between them is not surprising. However, for the case reported here, the coexistence region (the noisy region) is unusually large for liquid crystal (LC) materials (2K in temperature). For comparison, the coexistence window between the SmC_{α}^* phase and the SmC_{d6}^* phase of the same mixture was found to be about 0.4K [8].

More surprisingly however, is the fact that the phase coexistence in the noisy region happens on a microscopic level. The sub-μm scale immiscibility of the SmC_{d6}^* and the SmC_{d4}^* structure suggests a very large interface area in this region between the two structures. Normally the phase separation between two coexisting phases happens at a macroscopic scale in order to minimize the interface energy. The observed stable microscopic coexistence suggests an unusually low interface energy (surface tension) between the SmC_{d6}^* and the SmC_{d4}^* structure. Similar situations, where different orders coexist on a microscopic length scale, are found in microemulsions in surfactant systems [19], as well as in one of the recently identified

smectic blue phases (BP) [20, 21]. In all those situations, the observed structures result from a delicate balance between the ultralow interface tension (elasticity), mixing entropy, and the interactions involved.

Although we expect the physical origin of the noisy region structure to be similar to the situations discussed above, the many different competing interlayer interactions involved in AFLC materials (highly frustrated) make a complete understanding a uniquely interesting and theoretically challenging question. Meanwhile, the similar biaxial *distorted clock structures* of the two phases might provide a starting point for the understanding of the low interface energy.

As discussed above, structural elucidation for materials without long range order is a very challenging task. While substantial progress has been achieved for solid state systems [22], soft materials still prove to be very difficult to study. For example, the structure of the BP III in chiral LCs is still in heated debate decades after its discovery [23]. The high temperature (thus the degree of thermal fluctuation), small Q space involved all add up to the difficulties for scattering experiment in soft materials. In this aspect, our results also serve as a successful example and proof of principle how this task can be achieved even for partially ordered systems like AFLC, when appropriate technique is combined with computer simulations.

In summary, we report a detailed RXRD study of the temperature window between the newly discovered SmC_{d6}^* phase and the SmC_{d4}^* phase, which is characterized by multiple resonant peak spanning a wide Q_Z space. By careful analysis of the data and simulation based on the tensorial structural factor scheme, we came to an understanding of the noisy region as a coexistence region of the SmC_{d6}^* phase and the SmC_{d4}^* phase, with a percolating microscopic structure mixing on the sub-μm level. Our results will provide important information to the study of AFLC materials as well as the field of phase transitions. Also, as pointed out above, the noisy region presents an interesting example for the study of frustrated systems as well as a challenging state for the understanding of its thermodynamics and kinetics.

[1] A. Guinier, X-Ray Diffraction: In Crystals, Imperfect Crystals, and Amorphous Bodies (Courier Dover Publi-

cations, 1994).

[2] T. Egami and S. J. L. Billinge, Underneath the Bragg peaks: structural analysis of complex materials (Elsevier, 2003).

[3] H. Takezoe, E. Gorecka and M. Čepič, *Rev. Mod. Phys.* **82**, 897 (2010).

[4] J. P. F. Lagerwall and F. Giesselmann, *Chem. Phys. Chem* **7**, 20 (2006).

[5] LiDong Pan, B. K. McCoy, Shun Wang, Z. Q. Liu, S. T. Wang, R. Pindak, and C. C. Huang, *Phys. Rev. E* **83**, 060701 (2011).

[6] P. Mach, R. Pindak, A.-M. Levelut, P. Barois, H. T. Nguyen, C. C. Huang, and L. Furenlid, *Phys. Rev. Lett.* **81**, 1015 (1998).

[7] LiDong Pan, Shun Wang, C. S. Hsu, and C. C. Huang, *Phys. Rev. Lett.* **103**, 187802 (2009).

[8] Shun Wang, LiDong Pan, R. Pindak, Z. Q. Liu, H. T. Nguyen, and C. C. Huang, *Phys. Rev. Lett.* **104**, 027801 (2010).

[9] P. Mach, R. Pindak, A.-M. Levelut, P. Barois, H. T. Nguyen, H. Baltes, M. Hird, K. Toyne, A. Seed, J. W. Goodby, C. C. Huang, and L. Furenlid, *Phys. Rev. E* **60**, 6793 (1999).

[10] A.-M. Levelut and B. Pansu, *Phys. Rev. E* **60**, 6803 (1999).

[11] In the experiment, the layer plane is parallel to the film plate. The Z axis (direction of the x-ray photon's momentum transfer) is defined by the layer normal.

[12] Background contribution was obtained from the off resonant scan shown in Fig. 1.

[13] The data collection time in the noisy region was 4 sec.

[14] In principle, for a film with N layers, there are (N-1) in-dependent fitting parameters (azimuthal angle difference between neighboring layers). Thus for a film with several thousand layers, an exhaustive exploration in the parameter space is impractical.

[15] For general review of percolation models, see M. Sahimi, Applications of Percolation Model (Taylor & Francis, 1994).

[16] The main results of the simulations do not depend on the particular numerical choice of distortion angles or optical pitch. Here the value for the optical pitch and the distortion angle in the SmC_{d6}^* structure were adapted from fitting results in Ref. [8].

[17] Larger average correlation size in the nucleation model will result in more localized resonant peaks in the Q_Z space. For example, see Fig. 4(b) and the discussion in Ref [18].

[18] Similar results are observed with larger clusters for the percolation model. Note the percolation model with large nuclei clusters at 50% SmC_{d6}^* presents the same structure as the nucleation model with 50% SmC_{d6}^* u.c. with the same average nuclei size.

[19] For review, see Microemulsions: properties and applications, edited by M. Fanun (CRC Press, 2009).

[20] B. Pansu, E. Grelet, M. H. Li, and H. T. Nguyen, *Phys. Rev. E* **62**, 658 (2000).

[21] Jun Yamamoto, Isa Nishiyama, Miyoshi Inoue, and Hiroshi Yokoyama, *Nature* **437**, 525 (2005).

[22] Matthew J. Cliffe, Martin T. Dove, D. A. Drabold, and Andrew L. Goodwin, *Phys. Rev. Lett.* **104**, 125501 (2010), and the accompanying *Physics* Viewpoint article.

[23] O. Henrich, K. Stratford, M. E. Cates, and D. Marenduzzo, *Phys. Rev. Lett.* **106**, 107801 (2011).